1990

Selection of Friction Materials Used in Compact, High Performance Inverter Controlled Rotary Compressors

Y. Nakagawa
Hitachi Ltd.

Y. Kamitsuma
Hitachi Ltd.

T. Iizuka
Hitachi Ltd.

K. Ikeda
Hitachi Ltd.

SELECTION OF FRICTION MATERIALS USED IN COMPACT, HIGH PERFORMANCE INVERTER CONTROLLED ROTARY COMPRESSORS

Y. NAKAGAWA and Y. KAMITSUMA
Hitachi Research Laboratory
Hitachi, Ltd.
Hitachi-shi, Ibaraki-ken,
Japan, 317

T. IIZUKA and K. IKEDA
Tochigi Works
Hitachi, Ltd.
Shimotsuga-gun, Tochigi-ken,
Japan, 329-44

ABSTRACT

Since applications of rotary compressors driven by inverter motors have become more widespread, lubricating problems with the sliding parts have been appearing. The sliding parts require sufficient antiseizure and wear-resistant properties under the boundary lubricating conditions.

The authors have developed a new oxynitriding plus steam-treatment process. The surface of the material formed by the new process has an uppermost porous layer, which has a superior oil retaining property. Consequently, lubricating oil which penetrates and is held in the porous layer by capillary action, improves the lubricating ability in case of oil film breakdown.

Wear tests were made using a Suzuki-type abrasion testing machine with chloro fluoro carbon (CFC)-diluted refrigerating oil. Combinations of the new surface treated sliding members provided high reliability along with high antiseizure, and wear-resistant properties.

INTRODUCTION

Among the compressors that are used for air-conditioners, refrigerators and the like, there are several types including rotary, reciprocating, scroll, and screw types. The number of rotary compressors being used in air-conditioners and refrigerators has been rapidly increasing due to their higher efficiency, compacter size and lighter weight (Ref. 1). Compactness and high-output compressors of the variable speed control type are able to satisfy present trends for these appliances to have sophisticated functions.

Since applications of rolling-piston-type rotary compressors driven by inverter motors have become more widespread (Ref. 2), lubricating problems with their sliding parts have arisen. The rotation rates of inverter motors are quickly changed between 700-10,000 rpm, so their rotation modes are quite different from those of conventional rotary compressors. When the rotation rate is low and the pressure between the slides of the compressors is high, adhesive wear of the sliding members tends to occur because of breakdown of the oil film between the metal/metal boundaries. These are known as the boundary lubricating conditions.

Fig. 1 shows a sectional view of a typical rotary compressor. A rotary compressor is comprised of a rotatable crankshaft supported by an upper bearing and a lower bearing, a rotatable roller mounted on a crank pin of the crankshaft, a cylinder to accommodate the roller, and a slidable vane located within the vane slot formed in the cylinder. The distal end portion of the vane has a slide on the outer peripheral surface of the roller. In particular, consideration must be given to the distal end portion of the vane and the outer peripheral surface of the roller, the vane sides and the vane slot formed in the cylinder, and the shaft and bearings all of which receive the severest wear conditions.

In general, making the sliding members, e.g. crankshafts and vanes, of softnitrided or manganese-iron phosphated iron-based materials, is impractical at high speeds, because these materials lack sufficient antiseizure and wear-resistant properties. Therefore, in order to improve those characteristics under the boundary lubricating conditions, new combinations of materials are required.

In this paper, suitable combinations of materials to prevent abrasion through metal contact under the conditions with chloro fluoro carbon (CFC) dissolved in the lubricant oil are described.

SPECIMENS AND EXPERIMENTAL METHODS

Specimens

As shown in table 1, the specimens used in the experiments were a spheroidal graphite cast iron (FCD50), an eutectic graphite cast iron (FCC25), a molybdenum-nickel-chromium (Mo-Ni-Cr) cast iron and a high-speed tool steel (SKH51). FCC25, Mo-Ni-Cr cast iron and SKH51 specimens were preparing using their respective optimum heat treatments. FCD50, however, was used as cast. In Fig. 2, microstructures and Vickers hardness number of the four specimens are shown.

Optimum surface structure for tribology

Fig. 3 presents a schematic sectional view of one of the new surface structure models with sliding members for a spheroidal graphite cast iron under the boundary lubricaring conditions. As to an optimum surface structure for tribology when there is insufficient lubricating oil, several structures and material compositions were investigated. As a result, the best composition was obtained as having hard and porous layers. In these layers, the hard layer on the base metal prevents transformation of the surface due to metal contact. The porous layer, which is backed up by the hard layer, has a number of pores and cavities. Lubricating oil, accordingly, has penetrated into the porous layer by capillary action and is kept there where it improves the initial lubricating ability, or the lubricating ability in case of oil film breakdown. In order to obtain these layer structures, several surface modification methods were examined. Among them, an oxynitriding plus steam-treatment process was chosen, because it is easy to control this process, and it is economical and non-polluting. With this structure, the graphite surroundings are reinforced by the oxynitride layer, and portions of the graphite serve as solid lubrication holes and rigid oil retaining holes.

New surface treatment process

Sliding specimens of FCD50 and SKH51 were first subjected to an oxynitriding treatment in a gas mixture of ammonia gas and air (0.5-5.0 vol %), at 540°C for 0.25-3h, during which an oxynitride layer containing both granular iron oxide and iron nitride was formed on their surfaces. Then a steam-treatment was applied to this oxynitride layer (steam at 500-600°C for 1-4h) to produce an oxide film on it.

Measurement of oil spreading ratio

An oil drop (20 μℓ) was placed on the final oxide film (steam-treated, 500-600°C) and the area spreading rate of oil with time was measured. To do this the diameters of the oil drop, initially and after time passed were measured, and the area spreading ratio of oil was calculated (cf. insert Fig. 10).

Measurement of oil retained

Specimens having the oxide film formed by steam-treatment at 500-600°C, were kept 30 min. under vacuum (at a pressure of 10^{-1} Pa) to degas then, before being dropped into refrigerating oil which they absorbed for 5 min.

Scratch test method

The most important property of a surface treated film for tribology is its adhesion to the base metal. A simple and reliable adhesion test method is needed. Several techniques have been studied for adhesion testing (Refs. 3, 4). The scratch test method (Ref. 5) has been accepted as one of the better techniques. A schematic view of the scratch test is shown in Fig. 4. In the scratch test a diamond stylus is drawn over the specimen surface under a continuously increasing load until the film is detached. The film detachment can be observed using acoustic emission (AE) detectors to measure the high frequency vibrations caused by film detachment. The load on the indenter causing the film detachment is the critical normal force and it represents a comparative value of the film adhesion.

Seizure and wear test method

Most of the friction-material combinations were tested by a Suzuki-type abrasion testing machine (Fig. 5) where boundary lubricating takes place in low viscosity refrigerating oil diluted with CFC. Combinations included the new surface treated spheroidal graphite cast iron, high-speed tool steel and eutectic graphite, etc. Seizure load at rotation rates of 700-10,000 rpm, the friction coefficient and the wear volume loss were measured.

EXPERIMENTAL RESULTS

Surface structure with new treatment process

Figs. 6 and 7 show the surfaces and cross-sectional structures (Scanning Electron Microscopic images) of the oxide film on FCD50 and SKH51 formed by steam-treatment at 500-600°C. At 500°C, the surfaces of the oxide film have a number of fine cracks, and the cross-sectional structures are of fine columnar oxide. At 550 and 600°C, however, the oxide films have network structures containing a number of pores and cavities. Sizes of the pores and cavities in the oxide film formed at 600°C are larger than those at 550°C; this decreases the film strength of the former.

Fig. 8 shows the relationship between the thickness of the oxide film and either temperature or holding time of the steam-treatment process. The oxide film thickness increases with increased temperature or holding time of the steam-treatment process. The oxide film thickness of FCD50 is thicker than that of SKH51 which contains Cr, W, Mo and V (table 1).

Area spreading ratio of oxide film

Fig. 9 shows the relationship between the area spreading ratio of refrigerating oil diluted with CFC and the time required since the oil drop is placed on the oxide film. The area spreading ratio of oil increases with time. The oxide film formed by steam-treatment at 525°C has the highest area spreading ratio of oil. The area spreading ratio of oil for the non treated specimen does not change appreciably with time.

Fig. 10 sumarizes the area spreading ratio of oil 1 minute after the oil drop is placed on the oxide film. At 525 and 550°C, the area spreading ratio of oil has its maximum value. The oxide films formed by steam-treatment at these temperatures have a close affinity with the refrigerating oil.

Oil retention of oxide film

Fig. 11 describes oil retention by the oxide films formed by steam-treatments from 500-600°C. The amount of oil retained increases significantly from 500 to 525°C, but above 525°C the increase is slight. The oxide film formed by the steam-treatment process is composed mainly of porous iron oxide, Fe_3O_4, which has a good oil retention property, as well as chemical stability and corrosion resistance. Consequently, lubricating oil, which penetrated by capillary action and was retained in the porous iron oxide film, improves the lubricating ability in the case of the oil film breakdown.

Adhesive force of oxide film to base metal

Fig. 12 shows the relationship between the adhesion of the two different iron oxide films to the base metal as a function of the steam-treatment temperature. The adhesion of the iron oxide film formed by oxynitriding plus steam-treatment is superior to that of the oxide film formed only by the steam-treatment process. For oxynitriding plus steam-treatment above 525°C the critical normal force (i. e. adhesive force) is saturated, at about 15N.

Fig. 13 shows the distributions of constituent elements in the oxide film formed by steam-treatment only and by oxynitriding plus steam-treatment. For the steam-treated oxide film, the oxygen distribution is localized near the surface and drops sharply inside the film. By comparison, the oxygen distribution in the oxide film formed by oxynitriding plus steam-treatment is broader and drops more slowly on moving into the film. In this same film, the distribution of nitrogen increases on moving away from the surface up to a certain depth and then slowly decreases. For the oxynitriding plus steam-treatment, consequently, adhesion of the oxide layer to the oxynitriding layer is stronger than for the oxide film formed by steam-treatment alone, because oxygen and nitrogen distributions overlap in the surface layer.

Friction and wear characteristics of new surface treated materials

Fig. 14 shows the friction and wear characteristics of the new surface treated

(ONO) material combinations as measured by a Suzuki-type abrasion testing machine using refrigerating oil diluted with CFC. Characteristics of sulfu-nitrided (SN) (Ref. 6) material combinations are given for comparison. For the combinations of the new surface treated FCD50 or the new surface teated SKH51 and FCC25 or Mo-Ni-Cr cast iron, the wear volume is small and the friction coefficient decreases with increased sliding distance compared to sulfu-nitrided specimens.

Fig. 15 shows the effect of surface treatment methods on antiseizure properties combinations between the oxynitriding plus steam-treated FCD50 or the sulfu-nitrided FCD50 and hardened FCC25. At rotation rates of 2,000 rpm (2.5 m/s), the combination of the sulfu-nitrided FCD50 and FCC25 has a superior antiseizure property, the PV (the mathematical product of pressure and velocity) value is 17,000 $N/cm^2 \cdot m/s$. At rotation rates of 8,000 rpm (10 m/s), however, the combination of the new surface treated FCD50 and hardened FCC25 has a PV value greater than 10,000 $N/cm^2 \cdot m/s$; it is twice as high as the former combination.

Under field conditions, high reliability and efficiency are shown by the inverter compressor fabricated from a crankshaft made of the oxynitrided plus steam-treated or sulfu-nitrided spheroidal graphite cast iron, a blade made of the oxynitrided plus steam-treated high-speed tool steel, a roller made of hardened Mo-Ni-Cr cast iron, upper and lower bearings made of the steam-treated sintering iron, and a cylinder made of eutectic graphite cast iron.

CONCLUSIONS

Air-conditioners and refrigerators for domestic use have become more widespread since inverter control has been developed. Then, it is necessary to develop compressors of small size, light weight, a wide speed range, and low noise level. Lubricating problems with the sliding members of rotary compressors have arisen since the rotation rates of inverter motors are quickly changed between 700-10,000 rpm. When the rotation rate is low and the pressure between the sliding members is high, adhesive wear tends to occur because of metal contacts caused by transient breakdown of the oil film. These are known as the boundary lubricating conditions. Sliding members made of conventional surface treated iron based materials are not suitable at high speeds, the better antiseizure and wear resistant properties are needed under the boundary lubricating conditions. Therefore, the need for a new surface-treatment process was seen.

Optimum surface structure models with sliding parts were proposed. An oxynitriding process followed by a steam-treatment gave an iron oxide film on the surface of the oxynitriding layer. Adhesion of the iron oxide layer to the oxynitrided iron layer was improved. The oxidized iron layer was composed mainly of a porous Fe_3O_4 network, which is softer than the oxyinitrided layer. This uppermost porous layer had a superior oil retaining property because lubricating oil penetrated it and was held in the porous layer by capillary action. The oxynitriding layer prevented deformation of the surface of the sliding parts. Combinations of the new surface treated materials were tested by an abrasion testing machine where boundary lubricating took place using refrigerating oil diluted with CFC. Combinations of the new surface treated iron base metals had superior antiseizure properties, and both the friction coefficient and the wear volume loss were decreased.

An inverter compressor, fabricated from sliding members made of oxynitrided plus steam-treated or sulfu-nitrided spheroidal graphite cast iron and high-speed tool steel, demonstrated high reliability and efficiency under field conditions.

REFERENCES

1. K. Sekigami, et al.; Hitachi Review, 36 (1987), 169

2. Y. Serizawa, et al.; Hitachi Review, 36 (1987), 177

3. K. L. Mittal; Electrocomponent Sci. Technol., 3 (1976), 21

4. J. Valli, et al.; Surf. Eng., 2 (1986), 49

5. J. Valli, et al.; Wear, 115 (1987), 215

6. M. Marechal, et al.; Les Traitements de Surface Contre l Usure 23 (1968)

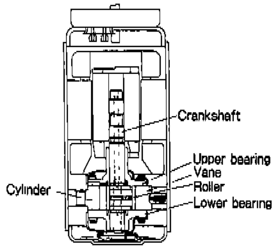

Fig. 1 A sectional view of rotary compressor

Table 1 Chemical compositions of specimens (%)

Element / Specimen	C	Si	Mn	P	S	Cr	Mo	Ni	Cu	Fe
FCD50	3.45	4.32	0.28	0.02	0.01	0.02	—	0.02	0.02	Bal.
FCC25	3.43	2.67	0.68	0.18	0.07	0.11	0.08	—	0.27	Bal.
Mo-Ni-Cr cast iron	3.35	2.10	0.72	0.25	0.09	0.75	0.28	0.30	—	Bal.
SKH51*	0.85	0.30	0.32	0.25	0.02	4.21	4.78	—	—	Bal.

* W : 6.32%, V : 2.15%

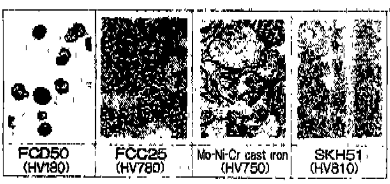

Fig. 2 Microstructures and Vickers hardness number (25 μm)

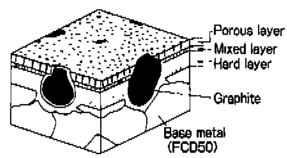

Fig. 3 A new model of surface structure

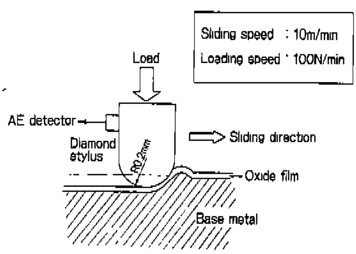

Fig. 4 A schematic view of scratch test

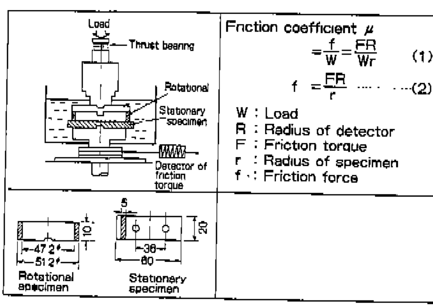

Fig. 5 A schematic view of a Suzuki-type abrasion machine

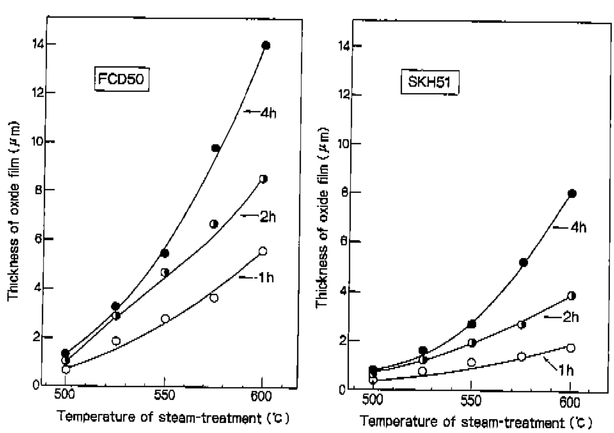

Fig. 8 Relationship between oxide film thickness and steam-treated temperature of FCD50 and SKH51

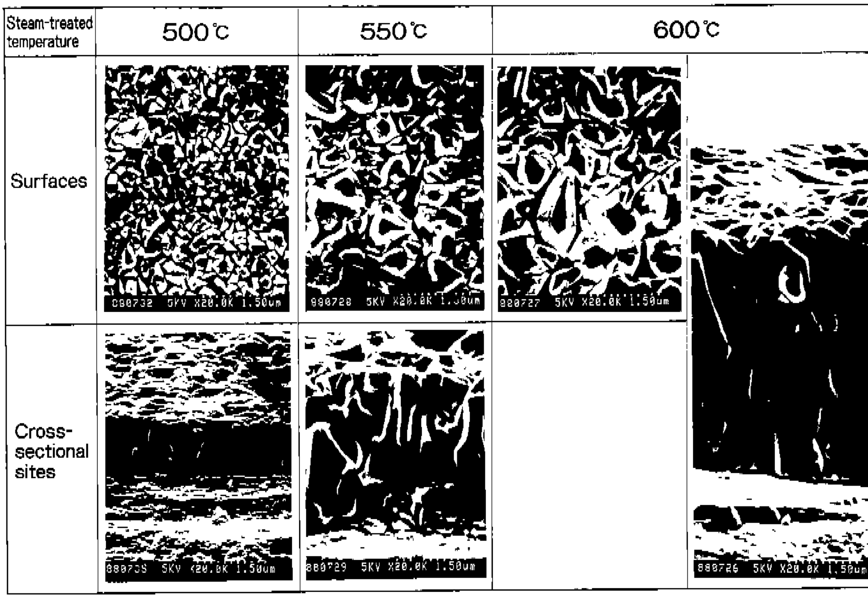

Fig. 6 Scanning electron microscopic images of oxide film (FCD50)

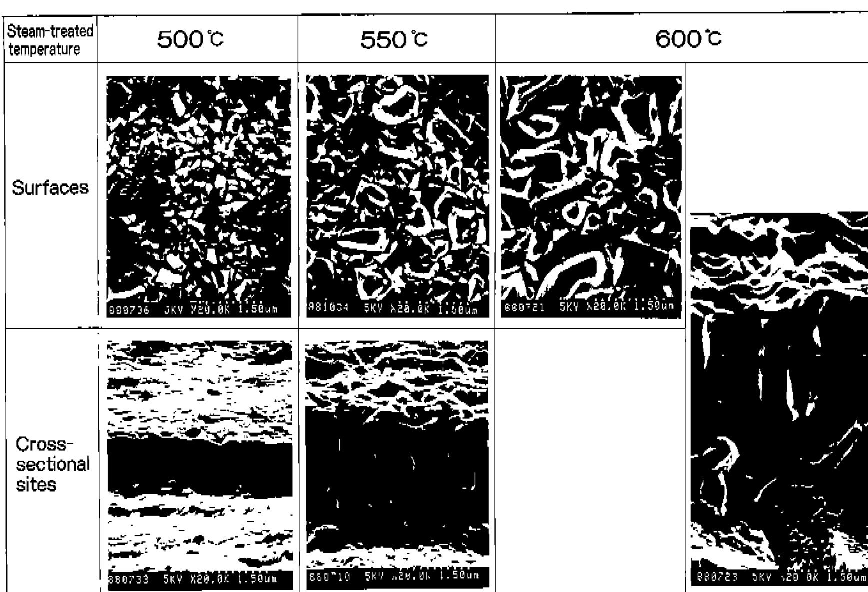

Fig. 7 Scanning electron microscopic images of oxide film (SKH51)

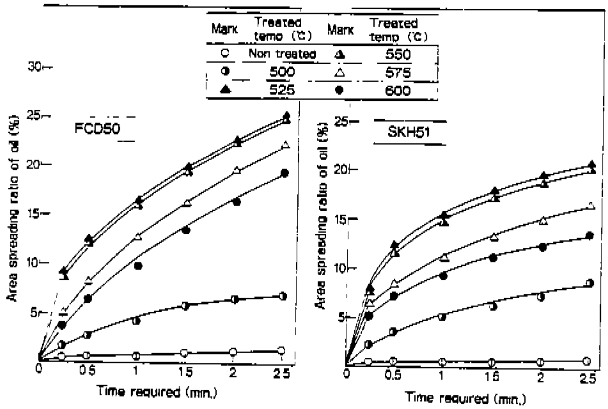

Fig. 9 Relationship between area spreading ratio of oil and time required since oil drop is placed on the oxide film

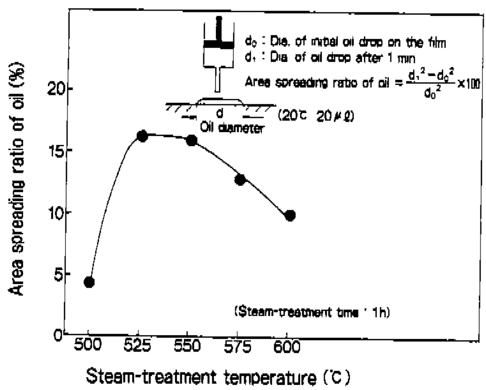

Fig. 10 Relationship between area spreading ratio of oil and steam-treatment temperature

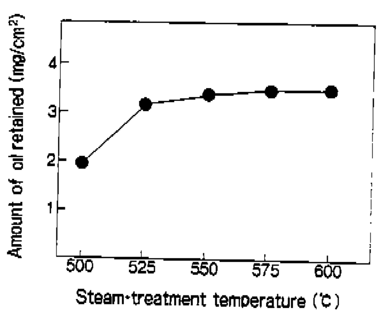

Fig. 11 Relationship between amount of oil retained and steam-treatment temperature (FCD50)

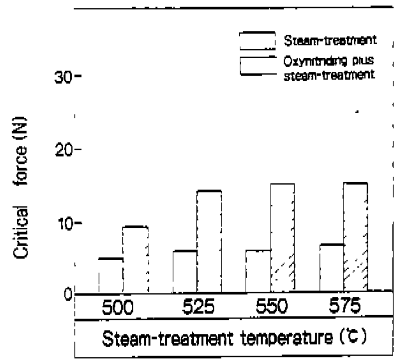

Fig.12 Influence of steam-treatment temperature on critical force of oxide film to base metal (FCD50)

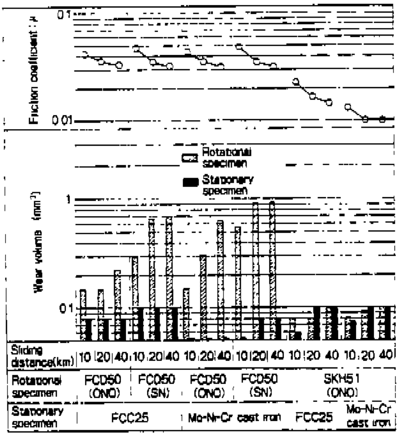

Fig.14 Friction-wear characteristics

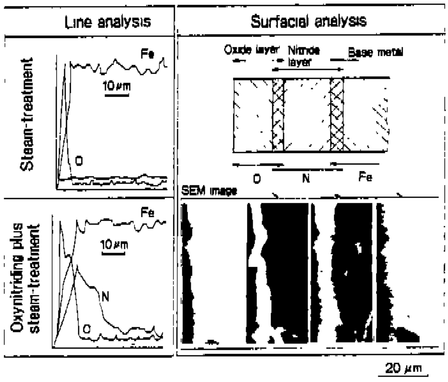

Fig.13 X-ray micro analysis of oxide film with steam-treatment and oxynitriding plus steam-treatment

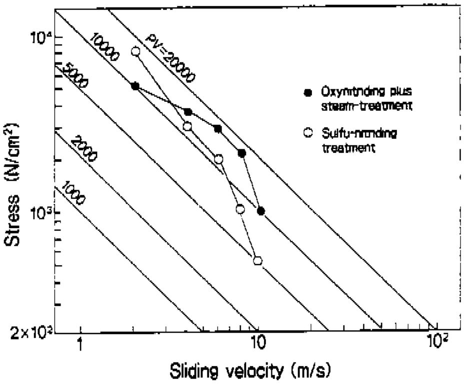

Fig.15 Influence of two surface treatments on seizure characteristics